IMPACT DEMAGNETIZATION OF THE MARTIAN CRUST: PRIMARIES VERSUS SECONDARIES.

N. Artemieva[1] , L. Hood[2] and B. A. Ivanov[1], [1]Institute for Dynamics of Geospheres, Moscow, artemeva@psi.edu, ivanov@idg.chph.ras.ru; [2]Lunar and Planetary Laboratory, University of Arizona, Tucson, lon@lpl.arizona.edu.

Introduction: The lack of magnetic anomalies within the giant martian impact basins, Hellas, Argyre, and Isidis is well-established by the Mars Global Surveyor magnetic data and has been estimated analytically [1.2]. In this paper we present numerical calculations of the shock wave decay in giant impacts, corresponding to formation of the martian basins and compare an input from direct impact and secondary impacts.

Numerical methods: To model formation of a large impact crater we use the two-dimensional SALEB code, originally developed by Amsden et al. [3] and recently modified by Ivanov [4]. The code is coupled with the ANEOS equation of state [5]. The modeled rock mechanics includes a strength model for intact and damaged rocks with gradual shear failure, an instant tension failure, dry friction for damaged rocks, the decrease of strength and internal friction close to melt temperature and shear strength increase with pressure increase. In addition to these familiar processes we also employ a model of acoustic fluidization [6].

Demagnetization by direct high-velocity impacts: The results of giant impact numerical simulations are shown in **Fig.1**. A 300-km-diameter projectile strikes vertically at 10 km/s. Transient cavity (TC) diameter is ~1130 km (probably, a bit larger than Agryre TC). Maximum shock compression drops rather quickly near the free surface: At a depth of 25 km (in the middle of a 50-km crust), it is below 1 GPa at a distance of 1000 km. It means that demagnetization is negligible beyond two TC radii.

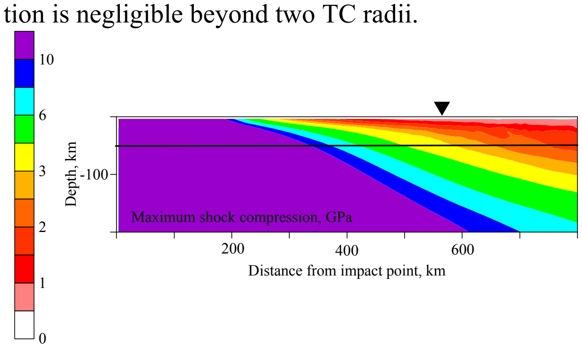

Fig. 1 Maximum shock pressure in the target after a 10 km/s, 300-km-diameter projectile impact. The black triangle shows the edge of the TC.

Demagnetization by low-velocity secondary impacts: All fragments ejected with velocity below escape (5 km/s) strike the surface at some distance from the primary crater, creating secondary craters, or, in the case of a very low velocity, boulders, on the surface. These secondary impacts not only substantially modify the surface, but may cause partial shock demagnetization of the crust. We calculate the ratio of a target volume V_t compressed above 1-1.5 GPa to a projectile volume V_{pr} for impacts with velocity U ranging from 1 to 4 km/s. The results are shown in **Fig. 2**. The maximum value of ~90 is for the highest impact velocity of 4 km/s, the minimum one is for a velocity of 1 km/s, and it is less than the projectile volume. This ratio may be approximated as follows: $V_t/V_{pr}=0.55*U^{3.66}$, where U is in km/s.

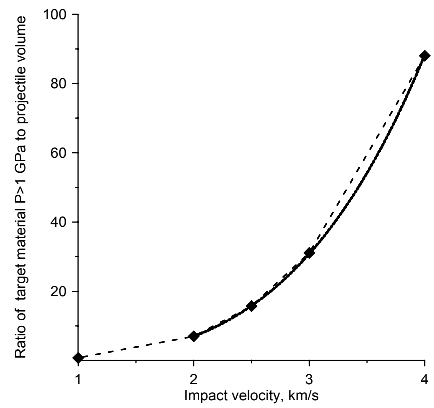

Fig. 2. Ratio of target material volume compressed above 1 GPa to projectile volume for impact velocities of 1-4 km/s.

Secondaries – Z-model: Ejection velocity U_{ej} at a distance r from an impact point is: $U_{ej}=U_*(r/R_{tr})^{-Z}$. U_* is a characteristic ejection velocity near the crater rim ($r=R_{tr}$), which may be defined as $(4/15gR_{tr})^{1/2}$ for a planet with gravity g. Z is a coefficient, which may be defined from experiments, or from comparison with numerical models [7]. It varies between about 2 near the axial stream tubes to about 4 near the surface, with Z=3 as a reasonable overall approximation (Melosh 1989). The total volume ejected through the free surface between r and $r+dr$ (the volume of a stream tube) is $dV=(\pi r^2)/2dr$. This material will be deposited within a ring with an inner radius $s=r+ U_{ej}^2/g$, assuming a ballistic trajectory and ejection angle of 45°, and a width of $ds=dr(1\text{-}2Z\ U_{ej}^2/gr)$. If all the material strikes the surface as a solid non-disrupted body, than we can estimate demagnetization of the crust as a function of distance from the impact site. The results are shown in **Fig.3** by dashed lines for 3 values of R_{tr}. The effect strongly depends on the transient cavity size: while transient cavity differs by a factor of two (655 km versus 1544 km), the thickness of demagnetization differs by an order of magnitude (7 km versus 73 km with the latter value exceeding the crust thickness). It is obvious that this estimate gives an upper limit of martian crustal demagnetization, as the real ejected volume consists of fragments of different sizes, which create separate (or overlapped) craters.

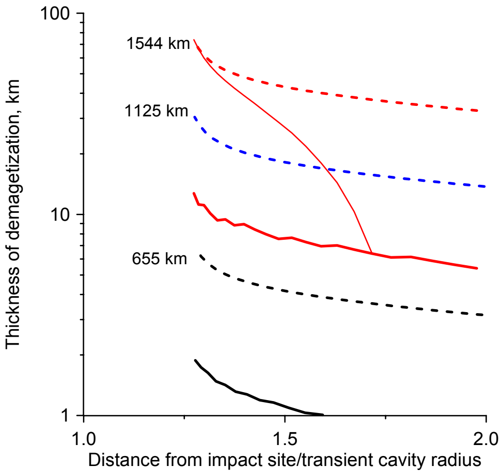

Fig. 3. Thickness of demagnetized crust (in km) as a function of distance from the impact point (measured in transient cavity radii). The corresponding transient cavity diameter is shown near each dashed line. Dashed lines show the upper limit of demagnetization (see text for details), thick solid lines – the lowest limit, and thin solid line for the largest basin is for a smooth interpolation between the two cases.

In this case, an important question is the fragments' size-frequency distribution (SFD). We use a standard distribution $N(m)=(m_{max}/m)^{-b}$, where m_{max} is the mass of the largest fragment, and b-coefficient commonly ranges between 0.8 and 0.9 for multiple fragmentation. A study of blocks on the rims of lunar craters ranging from a few meters to nearly 100 km in diameter yields a crude relation between maximum block size x_{max} (in meters) and crater diameter D (in meters): $x_{max}=(0.1\div 0.3)D^{2/3}$ [8]. Extrapolation to larger basins is not clear, as crater diameter itself is poorly defined and the size of the largest block depends on the crust structure (faulting, non-homogeneity, etc.). The 20 to 30-km diameter secondary craters associated with basin-forming impacts must have been produced by blocks (or, perhaps, by tight clusters of fragments) ranging from 3 to 4 km in diameter that were ejected at speeds of several kilometers per second. We assume that the largest fragment is ejected from the transient cavity edge with velocity U_* , and the maximum size is inversely proportional to the ejection velocity, i.e. $x_{max}(r)=x_{max}(R_{tr})U_*/U_{ej}$. [9]. We also assume that demagnetization in a given point is due to the largest fragments striking this area. Smaller fragments may give additional demagnetization, if they strike a non-demagnetized area, i.e. we estimate demagnetized volume starting from the largest impact until the point where the total effective area of demagnetization exceeds the landing area. Then we can find a thickness of demagnetization, dividing demagnetized volume by the ring area. The results are shown in **Fig.3** by solid lines. Undoubtedly, in this case, we have substantially weaker demagnetization – only the uppermost 12 km of the crust is demagnetized for the largest basin, and 2 km – for the smallest one. This estimate gives a lower limit of demagnetization by secondaries.

The real situation, most probably, is a combination of both estimates: In the far zone, separated fragments create well-separated secondary craters and demagnetize a thin upper layer of the crust (i.e. the lower limit gives correct answer); near the crater rim, tight clusters (with density close to density of non-disrupted target material) operate as a single solid impactor. A thin line for the largest basin (D_{tr}=1544 km) shows a smooth interpolation between the two zones.

Conclusions and future study: Outside the transient cavity, demagnetization by secondary impacts (SI) is at least comparable with demagnetization in a direct shock wave. While the direct shock wave cannot demagnetize the uppermost layers of the crust because of a quick decay near the free surface, secondary impacts demagnetize exactly these upper layers. The effectiveness of SI-demagnetization decreases sharply with crater size. It is negligible for basins smaller than ~500 km. The relative inputs from the primary shock wave and secondary impacts depend on the magnetic carriers distribution in the crust: If magnetic minerals are mainly in the uppermost layers, than secondaries may be of great importance.

References: [1] Hood L. et al. (2003). *GRL 30*, 1281, doi:10.1029/2002GL016657. [2] Mohit, P.S., J. Arkani-Hamed (2004) *Icarus 168*, 305-317.. [3] Amsden A. A. et al. (1980) *LNL Report LA-8095*. [4] Ivanov B. A. (2003) *Impact Cratering: Bridging the Gap Between Modeling and Observations*, Houston, TX abstr. 1155. [5] Thompson S. L. and H. S. Lauson (1972) *SNL Report SC-RR-71 0714*. [6] Melosh H. J. and B. A. Ivanov (1999) *Ann. Rev. Earth and Plan. Sci* 27, 385–415. [7] Maxwell D. E. (1977) In *Impact and Explosion Cratering*, 1003-1008. [8] Moore H. J. (1971). In *Analysis of Apollo 10 photography and visual observations*, 26-27. [9] Melosh H. J. (1989) *Impact cratering: A geologic process.* Oxford University Press. NY, 246 pp.